Mathematics

https://www.aimspress.com/journal/Math

AIMS Mathematics, 10(11): 27171–27190.
DOI: 10.3934/math.20251194
Received: 10 September 2025
Revised: 28 October 2025
Accepted: 13 November 2025
Published: 21 November 2025

Research article

A switching event-triggered control method for course tracking of surface vessels with output constraints and unknown control direction

Qian Gao[1] **and Jian Li**[2,*]

[1] School of Artificial Intelligence, Yantai Institute of Technology, Yantai 264005, China
[2] School of Mathematics and Information Sciences, Yantai University, Yantai 264005, China

* **Correspondence:** Email: ytulijian@ytu.edu.cn.

Abstract: This paper is devoted to the event-triggered course tracking control for a class of surface vessels (SVs). Notably, sampling of control input is considered under the coexistence of output constraint and unknown control direction, which is often overlooked in most related works. Other works often consider the sampling but ignore the output constraint. This leads to the inapplicability of traditional schemes on this topic. For this, two state transformations are first introduced for system output and reference signal, under which the boundedness of the new states implies the satisfaction of the output constraint. Then, two pivotal events are designed based on newly defined states, which facilitate the sampling mechanism of the controller and the updating mechanism of the controller parameters. By a skillful combination of the above two mechanisms, a switching event-triggered controller is explicitly designed, which guarantees that all the states of the resulting closed-loop system are bounded, while the system output practically tracks the reference signal, along with the satisfaction of the output constraint and the exclusion of the Zeno phenomenon. Finally, a simulation example is given to validate the effectiveness of the proposed theoretical results.

Keywords: surface vessel; course tracking; event-triggering; switching; output constraint
Mathematics Subject Classification: 93B52, 93C40

1. Introduction

Along with the wide application of surface vessels (SVs) in ocean engineering, such as in marine resource exploration, military mission execution, and environmental monitoring, considerable attention has been paid to the controls of SVs over the last decade, particularly in course tracking. Note that uncertainties, such as unknown parameters or external disturbances, are inherent in SV models, which pose significant challenges to course tracking control design. As a result, many control schemes have been proposed based on different assumptions on system uncertainties of SVs. For example, a robust integral backstepping method was proposed in [1] for course keeping of SV with known system parameters but without disturbance. An active disturbance rejection control algorithm and a robust method were proposed in [2] and [3], respectively, for an SV with known system parameters but unknown disturbance, while an adaptive method based on command filter was proposed in [4] for an SV with unknown parameters but free of disturbance. For some cases with more serious uncertainties, in which all the system parameters are unknown and external disturbance is allowed, course tracking control schemes based on fuzzy-logic, neural network, and reinforcement learning were proposed in [5–9], respectively. It is necessary to point out that all aforementioned works require the control direction (i.e., the sign of the control coefficient) to be known in advance. However, in certain situations, the control direction is unknown, which challenges the control problems. As an extension to this field, [10–13] proposed adaptive methods based on Nussbaum function for the course tracking control of SVs with unknown control directions.

In most practical cases, the output or states of SVs need to be kept in some compact set due to safety requirement or system specifications. Any violation of the constraints leads to unexpected responses, performance degradation, or even the breakdown of some equipments. Then, output or state constraints should be considered in the control of SVs; still, they are neglected in the above mentioned works (see [1–13]). In fact, course tracking of SVs with output or state constraints has been the focus of some investigations in recent years. Specifically, by introducing a logarithmic barrier Lyapunov function, adaptive heading tracking was solved for SVs with both full state constraints and unknown control direction in [14, 15], while adaptive neural network course tracking control was solved in [16] for SVs with output constraint but known control direction. In [17], by introducing a stochastic barrier Lyapunov function, nonsingular finite-time heading tracking control was solved under tracking error constraints.

Most of the above works consider the design of continuous-time controllers but disregard the sampling of the controllers. Hence, they are severely constrained on the saving of communication resource. In fact, along with the popular usage of engineering networks, controls based on event-triggered sampling mechanism have attracted a lot of attention due to their remarkable saving of limited network resources [18–21], but seldom for the course tracking of SVs. As a tentative work, event-triggered course tracking control was investigated in [5], but the output constraint was disregarded while the control direction had to be known, just as introduced above. Recognizing the constraints of the existing results, an interesting and nontrivial control problem arises, i.e., for some SVs with output constraint and unknown control direction, how to design an event-triggered course tracking controller?

Regarding the control problem raised above, this paper investigates the event-triggered course tracking control of a class of SVs with both output constraint and unknown control direction. Different from related works, where output constraint and unknown control direction are ignored, or only continuous time controllers are considered but their sampling is disregarded, in this paper, besides unknown system parameters (involving unknown control direction) and external disturbance, both output constraint and sampling of control input are considered. These remarkable characteristics result in an inapplicability of the traditional control methods on this topic. To solve the control problem, a switching event-triggered course tracking control scheme is proposed. Specifically, two state transformations are firstly introduced for system output and the reference signal, under which the boundedness of the new states guarantees the prescribed output constraint. Then, two pivotal events are skilfully chosen by using the transformed states, by which a switching event-triggered controller is explicitly designed, together with a triggered mechanism for the sampling of continuous time controller and a switching mechanism for the updating of controller parameters. Note that by the switching of two controller parameters in their respective candidate sequences, which are carefully chosen, the unknowns in control coefficient (including the unknown control direction) are compensated. Finally, a rigorous analysis procedure is given to show that, along with the exclusion of the Zeno phenomenon and the stopping of the switching of the controller parameters, all the states of the resulting closed-loop system are bounded, while the system output practically tracks the reference signal without any violation of the output constraint.

In the following, we highlight the main contributions of the paper by specifying the distinguishable characteristics of the system and analyzing the principal difficulties of the control problem:

1) *Unknown control direction is allowed simultaneously with output constraint.* Different from the related works where control direction must be known or output constraint is neglected, both unknown control direction and output constraint are considered in the paper, which leads to the inapplicability of the traditional control schemes. Then, certain mechanisms for the compensation of unknown control direction and the assurance of output constraint should be developed and then incorporated into the control design.

2) *Sampling based on event-triggered mechanism is considered.* Different from most of the related works, which disregard the sampling of the controllers or are constrained by the severe assumptions on control direction and output constraint, sampling of control input is considered under the presence of unknown control direction and output constraint. Thus, an event-triggered mechanism should be designed for the sampling of control input, which challenges the control design and performance analysis.

The remaining parts of the paper are organized as follows: Section 2 formulates the control problem investigated in the paper. Section 3 presents the procedure of control design. Section 4 brings the performance analysis of the resulting closed-loop system. Section 5 gives a numerical example to verify the effectiveness of the proposed theoretical results. This paper ends with Section 6, which gives some concluding remarks.

2. Problem formulation

In this paper, course tracking control is investigated for the following Norrbin nonlinear ship model, which describes the steering dynamics of a ship:

$$T\ddot{\Psi} + \dot{\Psi} + \alpha\dot{\Psi}^3 = K(\delta + \delta_w), \tag{2.1}$$

where Ψ is the course angle, δ is the actual control rudder angle, δ_w represents the equivalent rudder angle induced by environmental disturbances, T is the unknown time constant, K is the unknown gain constant, and α is the unknown Norrbin coefficient.

To facilitate the subsequent control design, equation (2.1) is transformed by defining the following state variables: $x_1 = \Psi$, $x_2 = \dot{\Psi}$. Then, the following system in state space is obtained from (2.1):

$$\begin{cases} \dot{x}_1 = x_2, \\ \dot{x}_2 = \theta_0 U + \sum_{j=1}^{2} \theta_j \varphi_{2,j}(x_2) + d(t), \\ y = x_1, \end{cases} \tag{2.2}$$

where $\theta_0 = \frac{K}{T}$, referred to as the control coefficient, is an unknown constant with unknown size and sign, while $\theta_1 = -\frac{1}{T}$ and $\theta_2 = -\frac{\alpha}{T}$ are unknown constants, $d(t) = \theta_0\delta_w$ is an unknown bounded external disturbance, $\varphi_{2,1}(x_2) = x_2$, $\varphi_{2,2}(x_2) = x_2^3$ are known nonlinear functions, y is the system output and $u = \delta$ is the control input.

The control objective of the paper is to design an event-trigged controller to ensure that all the states of the closed-loop system are bounded; moreover, the output y practically tracks the reference signal y_r while satisfying the output constraint $k_l(t) \leq y \leq k_u(t)$, $t \geq 0$, with k_l and k_u being some time-varying functions satisfying Assumptions 2.3-2.5 below.

Some assumptions about external disturbances, reference signal, and the output constraints are given as follows:

Assumption 2.1. There exists an unknown constant $\bar{d}$ such that $|d| \leq \bar{d}$.

Assumption 2.2. There exists an unknown constant $\bar{y}_r$ such that $|y_r| + |\dot{y}_r| \leq \bar{y}_r$.

Assumption 2.3. There exist some functions $k_{l,m}(t)$ and $k_{u,m}(t)$ such that $k_l(t) < k_{l,m}(t) \leq y_r(t) \leq k_{u,m}(t) < k_u(t)$, $t \geq 0$.

Assumption 2.4. There exists a constant $\bar{k}$ such that $|k_l| + |\dot{k}_l| \leq \bar{k}$, $|k_u| + |\dot{k}_u| \leq \bar{k}$.

Assumption 2.5. There exist some positive constants $\varepsilon_1, \varepsilon_2 > 0$ such that $k_{l,m}(t) - k_l(t) \geq \varepsilon_1$, $k_u(t) - k_{u,m}(t) \geq \varepsilon_2$, $t \geq 0$.

Remark 2.1. The above five assumptions are meaningful in practice and necessary for the later control design and performance analysis. Specifically, Assumption 2.1 shows that the disturbance has an unknown upper bound. In practice, the influence from the external environment on the system (usually treated as the disturbance) is finite, and therefore bounded. Assumptions 2.2 and 2.4 show that the reference signal and the output constraint functions, as well as their time derivatives are bounded by unknown constants, which are routine for the tracking control with output constraint. In most of the cases, the reference signal and the output constraints are given as the trajectories of some moving targets. Then, their positions (i.e., y_r, k_l, k_u) and the velocities (i.e., $\dot{y}_r$, $\dot{k}_l$, $\dot{k}_u$) are usually bounded. Assumptions 2.3 and 2.5 shows that the reference signal must satisfy the constraint that lies within the output constraint. This is meaningful in practice since one cannot track some reference signals that exceed the prescribed output constraint.

3. Control design

3.1. Transformations for system output and reference signal

To overcome the output constraint, transformations for system output and reference signal are introduced. First, the transformation for system output y is defined as follows:

$$\xi = \frac{1}{2}\left(\frac{1 + k_u y}{k_u - y} - \frac{1 + k_l y}{y - k_l}\right). \tag{3.1}$$

Then, by direct computation, the transformed state ξ satisfies the following dynamics:

$$\dot{\xi} = \psi\dot{y} + w,$$

with

$$\begin{cases} \psi &= \frac{k_l^2+1}{2(y-k_l)^2} + \frac{k_u^2+1}{2(k_u-y)^2}, \\ w &= w_1\dot{k}_l - w_2\dot{k}_u, \\ w_1 &= \frac{y^2+1}{2(y-k_l)^2}, \\ w_2 &= \frac{y^2+1}{2(k_u-y)^2}. \end{cases}$$

Second, the transformation for reference signal y_r is defined as follows:

$$\eta = \frac{1}{2}\left(\frac{1 + k_u y_r}{k_u - y_r} - \frac{1 + k_l y_r}{y_r - k_l}\right), \tag{3.2}$$

which clearly satisfies the following dynamics by the similar computation as that for ξ:

$$\dot{\eta} \;\; = \;\; \bar{\psi}\dot{y}_r + \bar{w}, \tag{3.3}$$

with

$$\begin{cases} \bar{\psi} &= \frac{k_l^2+1}{2(y_r-k_l)^2} + \frac{k_u^2+1}{2(k_u-y_r)^2}, \\ \bar{w} &= \bar{w}_1\dot{k}_l - \bar{w}_2\dot{k}_u, \\ \bar{w}_1 &= \frac{y_r^2+1}{2(y_r-k_l)^2}, \\ \bar{w}_2 &= \frac{y_r^2+1}{2(k_u-y_r)^2}. \end{cases}$$

In the following, some discussions are given for the two transformations given above which will be used in the later control design and performance analysis.

1) From (3.1), the transformed output ξ will tend to infinity as original output y (i.e., x_1) reaches to one boundary of the output constraint, i.e., for some initial output that satisfies the output constraint $k_l(0) \leq y(0) \leq k_u(0)$, $\xi \to \infty$ if and only if $y \to k_l$ or $y \to k_u$. Then, the output constraint can be guaranteed by the boundedness of the transformed output ξ.

2) From (3.2), while noting the boundedness of the reference signal and constrained functions we can obtain the boundedness of the transformed reference signal η and its derivative $\dot{\eta}$. Specifically, by Assumptions 2.3 and 2.5, we directly obtain that

$$\begin{cases} 0 < \frac{1}{k_u-k_l} < \frac{1}{y_r-k_l} < \frac{1}{k_{l,m}-k_l} \leq \frac{1}{\varepsilon_1}, \\ 0 < \frac{1}{k_u-k_l} < \frac{1}{k_u-y_r} < \frac{1}{k_u-k_{u,m}} \leq \frac{1}{\varepsilon_2}. \end{cases}$$

This, together with Assumptions 2.2 and 2.4, gives that

$$|\eta| \leq \frac{\bar{k}\bar{y}_r + 1}{2}\left(\frac{1}{\varepsilon_1} + \frac{1}{\varepsilon_2}\right),$$

which gives the boundedness of η. By a similar derivation, we can also obtain the boundedness of $\dot{\eta}$. Then, there is a positive constant $\bar{\eta}$ such that

$$|\eta| + |\dot{\eta}| \leq \bar{\eta}. \tag{3.4}$$

3.2. Control design

In this section, a switching event-triggered control design procedure is given. First, by the transformed states ξ and η as well as the original state x_2, we define the following state transformation:

$$\begin{cases} z_1 = \xi - \eta, \\ z_2 = x_2 - \alpha_1, \end{cases} \tag{3.5}$$

where

$$\alpha_1(x_1, k_l, k_u, y_r) = -\hat{c}_1 z_1 \psi^{-1}\left(1 + w_1^2 + w_2^2\right), \tag{3.6}$$

with $\hat{c}_1$ (and $\hat{c}_2$ appears later) being some controller parameters, which will be tuned based on certain switching mechanisms given below. Then, by the above new state, we define the following two pivotal events:

$$\begin{cases} \textbf{Event ①} : z_1(t)^2 + z_2(t)^2 > (z_1(t'_s)^2 + z_2(t'_s)^2)e^{t'_s - t} + \frac{\varepsilon^2}{32\bar{k}^4}, \\ \textbf{Event ②} : |U(t) - \alpha_2(x_1, x_2, k_l, k_u, y_r, \hat{c}_1, \hat{c}_2)| \geq \delta, \end{cases} \tag{3.7}$$

where δ is some positive constant and α_2 is defined as follows:

$$\alpha_2(x_1, x_2, k_l, k_u, y_r, \hat{c}_1, \hat{c}_2) = -\hat{c}_2(1 + \Lambda)z_2, \tag{3.8}$$

with Λ being chosen as follows:

$$\begin{aligned} \Lambda = {} & \psi^2 + 2 + \sum_{j=1}^{2} \varphi_{2,j}^2 + \Big(\frac{\partial \alpha_1}{\partial y_r}\Big)^2 + \Big(\frac{\partial \alpha_1}{\partial k_l}\Big)^2 + \Big(\frac{\partial \alpha_1}{\partial k_u}\Big)^2 + \Big(\frac{\partial \alpha_1}{\partial x_1}\Big)^2 \\ & + \hat{c}_1^2(\psi^{-1})^2\Big(\frac{\partial \alpha_1}{\partial x_1}\Big)^2 + \Big(\frac{\partial \alpha_1}{\partial x_1}\Big)^2(\psi^{-1})^2(w_1^2 + w_2^2)^2. \end{aligned}$$

Remark 3.1. From the first line of (3.5) that, z_1 can be viewed as the transformed tracking error constructed by two transformed signals ξ, η. In fact, based on transformations (3.1) and (3.2), the relationship between the transformed tracking error and the original one can be explicitly shown as follows:

$$z_1 = \Phi(t)(x_1 - y_r), \tag{3.9}$$

with

$$\Phi(t) = \frac{1}{2}\left(\frac{k_l^2 + 1}{(y - k_l)(y_r - k_l)} + \frac{k_u^2 + 1}{(k_u - y)(k_u - y_r)}\right). \tag{3.10}$$

Such relationship will be used in the later performance analysis.

We are now in a position to present the controller for system (2.2), which is defined as follows:

$$U(t) = \alpha_2\Big(x_1(t_k), x_2(t_k), k_l(t_k), k_u(t_k), y_r(t_k), \hat{c}_1(t'_{m,k}), \hat{c}_2(t'_{m,k})\Big), \ t \in [t_k, t_{k+1}), \tag{3.11}$$

where t_k ($t_1 = 0$), and the time at which the controller is sampled, is tuned online by the following event-triggered sampling mechanism:

$$t_{k+1} = \inf\left\{t > t_k | \text{At time } t, \text{either } \textbf{Event ① or Event ②} \text{ happens}, t'_s = t'_{m,k}\right\}, \tag{3.12}$$

$t'_{m,k}$ is defined as

$$\begin{cases} t'_{m,k} = t'_m, \\ m = \arg \underset{s}{max}\, t'_s \leq t_k, \end{cases} \tag{3.13}$$

with t'_s ($t'_1 = 0$), and the time at which two controller parameters $\hat{c}_1$, $\hat{c}_2$ update, being updated with $\hat{c}_1$, $\hat{c}_2$ by the following switching mechanism:

$$\begin{cases} t'_{s+1} = \inf\left\{t > t'_s | \text{At time } t, \textbf{Event ①} \text{ happens}\right\}, \\ \hat{c}_1(t'_s) = C_{1,s}, \quad \hat{c}_2(t'_s) = C_{2,s}, \end{cases} \tag{3.14}$$

where $\{C_{i,s} | s \in \mathbb{N}\}$, $i = 1, 2$ are two sequences that are chosen to satisfy that

$$\begin{cases} \begin{cases} 1 \leq C_{1,s} \leq C_{1,s+1}, \\ \lim\limits_{s \to +\infty} C_{1,s} = +\infty, \end{cases} \\ \begin{cases} 0 \leq |C_{2,s}| \leq |C_{2,s+1}|, \\ \lim\limits_{s \to +\infty} |C_{2,s}| = +\infty, \\ \textbf{sign}(C_{2,s}) = -\textbf{sign}(C_{2,s+1}). \end{cases} \end{cases} \tag{3.15}$$

Remark 3.2. As mentioned above, three important times, i.e., t_k, t'_s and $t'_{m,k}$, are used in control design. Seeing from (3.12) and (3.14), t_k and t'_s denote the times at which the controller is sampled and the controller parameters therein update, respectively, while (3.13) shows that $t'_{m,k}$ denotes the final switching time before the sampling time t_k. The relationship of these three times is shown in Figure 1.

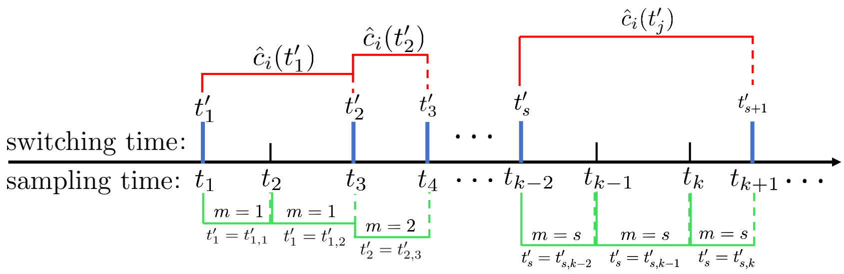

Figure 1. Relationship among three important times t_k, t'_s, and $t'_{m,k}$.

Remark 3.3. The two events given by (3.7) are designed independently and play different roles in control design. Specifically, **Event ①** is designed based on the desirable control performance (i.e., the boundedness of system signals and the practical tracking performance), which is used to update both the sampling times of control input and the switching times of controller parameters (as shown respectively by (3.12) and (3.14)). **Event ②** is designed based on the sampling error, together with a static threshold (i.e., δ), which is only used to update the sampling times (as shown by (3.12)). By a skillful combination of these two events, both the sampling and switching mechanisms are given.

Remark 3.4. As shown in Figure 1, with the sampling and switching mechanisms (given by (3.12) and (3.14), respectively), both sampling and switching happen once **Event ①** happens. Then, at switching times t'_s, sampling of control input also happens. Thus, for the sequences of switching times and sampling times, denoted respectively by $\{t'_s\}$ and $\{t_k\}$, there holds that $\{t'_s\} \subseteq \{t_k\}$. This implies that, for each sampling interval $[t_k, t_{k+1})$, there exists a switching interval $[t'_s, t'_{s+1})$ such that $[t_k, t_{k+1}) \subseteq [t'_s, t'_{s+1})$. Such relationship will be used in the later performance analysis.

Remark 3.5. The sequences $\{C_{i,s} | s \in \mathbb{N}\}$, $i = 1, 2$, which satisfy conditions (3.15), can be explicitly constructed off-line, such as

$$\begin{cases} C_{1,s} & : \; 1, 2, 3, 4, \cdots, s, \cdots \\ C_{2,s} & : \; 1, -2, 3, -4, \cdots, (-1)^{s-1}s, \cdots \end{cases} \tag{3.16}$$

Proposition 3.1. For system (2.2), the designed switching event-triggered controller (3.11) with event-triggered sampling mechanism (3.12) and switching mechanism (3.14) guarantees that the Lyapunov function $V = \frac{1}{2}(z_1^2 + z_2^2)$ satisfies the following inequality on each sampling interval $[t_k, t_{k+1})$:

$$\dot{V} \le -(\hat{c}_1 - 3)z_1^2 - (\hat{c}_1 - 1)z_1^2(w_1^2 + w_2^2) - (\hat{c}_2\theta_0 - 1)z_2^2\Lambda - \hat{c}_2\theta_0 z_2^2 + M, \tag{3.17}$$

with M being some positive constant.

Proof. Such a proposition is proved by the following 2-step recursive procedure.

Step 1: Define $V_1 = \frac{1}{2}z_1^2$. Then, along the solutions of system (2.2), $\dot{V}_1$ is defined as follows:

$$\begin{aligned} \dot{V}_1 &= z_1(\psi \dot{x}_1 + w - \dot{\eta}) \\ &= z_1(\psi z_2 + \psi\alpha_1 + w - \dot{\eta}). \end{aligned} \tag{3.18}$$

Noting the definition of w and using Assumption 2.4, Young's inequality gives that

$$\begin{aligned} z_1(w - \dot{\eta}) &= z_1(w_1\dot{k}_l + w_2\dot{k}_u - \dot{\eta}) \\ &\le z_1^2(w_1^2 + w_2^2 + 1) + \dot{k}_l^2 + \dot{k}_u^2 + \dot{\eta}^2 \\ &\le z_1^2(w_1^2 + w_2^2 + 1) + \bar{M}_1, \end{aligned}$$

with $\bar{M}_1 = 2\bar{k}^2 + \bar{\eta}^2$. Substituting the above inequality into (3.18) leads to

$$\dot{V}_1 \le z_1\left(\psi z_2 + \psi\alpha_1 + z_1(w_1^2 + w_2^2)\right) + \bar{M}_1.$$

Then, by the choice of α_1 which is given in (3.6), we obtain that

$$\dot{V}_1 \le -\hat{c}_1 z_1^2 - (\hat{c}_1 - 1)z_1^2(w_1^2 + w_2^2) + z_1\psi z_2 + \bar{M}_1. \tag{3.19}$$

Step 2: Define $V = V_1 + \frac{1}{2}z_2^2$. Noting the definition of α_1 given in (3.6), we directly obtain that

$$\begin{aligned} \dot{\alpha}_1 &= \frac{\partial\alpha_1}{\partial x_1}\dot{x}_1 + \frac{\partial\alpha_1}{\partial y_r}\dot{y}_r + \frac{\partial\alpha_1}{\partial k_l}\dot{k}_l + \frac{\partial\alpha_1}{\partial k_u}\dot{k}_u \\ &= \frac{\partial\alpha_1}{\partial x_1}(z_2 + \alpha_1) + \frac{\partial\alpha_1}{\partial y_r}\dot{y}_r + \frac{\partial\alpha_1}{\partial k_l}\dot{k}_l + \frac{\partial\alpha_1}{\partial k_u}\dot{k}_u. \end{aligned} \tag{3.20}$$

Then, along the solutions of system (2.2), $\dot{V}_2$ is given as follows:

$$\begin{aligned}\dot{V} &\leq -\hat{c}_1 z_1^2 - (\hat{c}_1 - 1) z_1^2 (w_1^2 + w_2^2) + z_1 \psi z_2 + \bar{M}_1 + z_2(\dot{x}_2 - \dot{\alpha}_1)\\ &\leq -\hat{c}_1 z_1^2 - (\hat{c}_1 - 1) z_1^2 (w_1^2 + w_2^2) + \bar{M}_1^2 + z_2\Big(\psi z_1 + \theta_0(U - \alpha_2) + \theta_0 \alpha_2\\ &\quad + \sum_{j=1}^{2} \theta_j \varphi_{2,j}(x_2) + d - \frac{\partial \alpha_1}{\partial x_1}(z_2 + \alpha_1) - \frac{\partial \alpha_1}{\partial y_r}\dot{y}_r - \frac{\partial \alpha_1}{\partial k_l}\dot{k}_l - \frac{\partial \alpha_1}{\partial k_u}\dot{k}_u\Big).\end{aligned} \tag{3.21}$$

Some terms on the right-hand side of (3.21) should be estimated for the later control design. Specifically, by Assumptions 2.1, 2.2, and 2.4 while using Young's inequality, we have

$$\begin{cases} z_2 \psi z_1 \leq z_1^2 + \psi^2 z_2^2,\\ z_2 \sum_{j=1}^{2} \theta_j \varphi_{2,j}(x_2) \leq z_2^2 \sum_{j=1}^{2} \varphi_{2,j}^2(x_2) + \theta_1^2 + \theta_2^2,\\ z_2 d \leq z_2^2 + \bar{d}^2,\\ -z_2 \frac{\partial \alpha_1}{\partial y_r}\dot{y}_r \leq z_2^2 \left(\frac{\partial \alpha_1}{\partial y_r}\right)^2 + \bar{y}_r^2,\\ -z_2\Big(\frac{\partial \alpha_1}{\partial k_l}\dot{k}_l + \frac{\partial \alpha_1}{\partial k_u}\dot{k}_u\Big) \leq z_2^2 \left(\left(\frac{\partial \alpha_1}{\partial k_l}\right)^2 + \left(\frac{\partial \alpha_1}{\partial k_u}\right)^2\right) + 2\bar{k}^2,\\ -z_2 \frac{\partial \alpha_1}{\partial x_1}\left(z_2 - \hat{c}_1 \psi^{-1} z_1 - \psi^{-1} z_1 (w_1 + w_2)\right)\\ \quad \leq z_2^2 \left(\left(\frac{\partial \alpha_1}{\partial x_1}\right)^2 + 1\right) + z_2^2 \hat{c}_1^2 (\psi^{-1})^2 \Big(\frac{\partial \alpha_1}{\partial x_1}\Big)^2 + z_2^2 \Big(\frac{\partial \alpha_1}{\partial x_1}\Big)^2 (\psi^{-1})^2 (w_1^2 + w_2^2) + 2 z_1^2. \end{cases} \tag{3.22}$$

Moreover, by the sampling mechanism (3.12), on the sampling interval $[t_k, t_{k+1})$, **Event ①** does not happen, and hence $|U - \alpha_2| \leq \delta$. Thus, we obtain that

$$z_2 \theta_0 (U - \alpha_2) \leq z_2^2 + \theta_0^2 |U - \alpha_2|^2 \quad \leq z_2^2 + \theta_0^2 \delta^2. \tag{3.23}$$

Substituting (3.22) and (3.23) into (3.21) leads to that

$$\begin{aligned}\dot{V} &\leq -(\hat{c}_1 - 3) z_1^2 - (\hat{c}_1 - 1) z_1^2 (w_1^2 + w_2^2) + z_2\Big(\psi^2 z_2 + 2 z_2 + z_2 \sum_{j=1}^{2} \varphi_{2,j}^2(x_2)\\ &\quad + z_2\left(\Big(\frac{\partial \alpha_1}{\partial y_r}\Big)^2 + \Big(\frac{\partial \alpha_1}{\partial k_l}\Big)^2 + \Big(\frac{\partial \alpha_1}{\partial k_u}\Big)^2 + \frac{\partial \alpha_1}{\partial x_1}\right)\\ &\quad + z_2 \hat{c}_1^2 (\psi^{-1})^2 \Big(\frac{\partial \alpha_1}{\partial x_1}\Big)^2 + z_2 \Big(\frac{\partial \alpha_1}{\partial x_1}\Big)^2 (\psi^{-1})^2 (w_1^2 + w_2^2)^2 + \theta_0 \alpha_2\Big)\\ &\quad + 4\bar{k}^2 + \theta_0^2 \delta^2 + \theta_1^2 + \theta_2^2 + \bar{d}^2 + \bar{y}_r^2\\ &\leq -(\hat{c}_1 - 3) z_1^2 - (\hat{c}_1 - 1) z_1^2 (w_1^2 + w_2^2) + M + z_2^2 \Lambda + \theta_0 z_2 \alpha_2,\end{aligned}$$

with $M = 4\bar{k}^2 + \theta_0^2 \delta^2 + \theta_1^2 + \theta_2^2 + \bar{d}^2 + \bar{y}_r^2$, Then, substituting α_2 as given by (3.8) leads to (3.17). This completes the proof. □

4. Performance analysis

This section gives the performance analysis of the resulting closed-loop system. First, two propositions are given (i.e., Propositions 4.1 and 4.2 below) to prepare for the presentation of the main results. Specifically, Proposition 4.1 gives the results based on Lyapunov analysis, whose proof is omitted since it is direct from Proposition 3.1. Proposition 4.2 provides an important property of the switching mechanism. Then, one theorem (i.e., Theorem 4.1) is given to summarize the proposed main results and provide the detailed proof.

Proposition 4.1. On $[t_k, t_{k+1})$, once $\hat{c}_1 = C_{1,k}$, $\hat{c}_2 = C_{2,k}$ such that

$$\begin{cases} \hat{c}_1 > \frac{32\bar{k}^4 M}{\varepsilon^2} + \frac{7}{2}, \\ \theta_0 \hat{c}_2 > \frac{32\bar{k}^4 M}{\varepsilon^2} + \frac{3}{2}, \end{cases} \tag{4.1}$$

then, the event-triggered controller guarantees that Lyapunov function V satisfies that

$$\dot{V} \leq -\mu V + M, \tag{4.2}$$

with $\mu = \min\{2(\hat{c}_1 - 3), 2\hat{c}_2\theta_0\}$.

Proposition 4.2. Under switching mechanism (3.14), the switching of controller parameters $\hat{c}_1$, $\hat{c}_2$ happens a finite number of times.

Proof. This proposition is proved by contradiction. Suppose that the switching of controller parameters $\hat{c}_1$, $\hat{c}_2$ happens an infinite number of times. Then, based on the switching mechanism (3.14) and the conditions that the sequences $\{C_{i,s} | s \in \mathbb{N}\}$ satisfy (given by (3.15)), there is a switching interval $[t'_{s^*}, t'_{s^*+1})$, on which $\hat{c}_1 = C_{1,s^*}$ is larger than an arbitrary constant (which implies the first inequality of (4.1)), and meanwhile, $\hat{c}_2 = C_{2,s^*}$ has the same sign as θ_0, while its product with θ_0 is larger than an arbitrary constant (which implies the second inequality of (4.1)). Thus, by Proposition 4.1, (4.2) holds.

Integrating both sides of (4.2) on $[t'_{s^*}, t'_{s^*+1}]$, while noting the definition of μ with (4.1) given above, leads to

$$\begin{aligned} z_1(t'_{s^*+1})^2 + z_2(t'_{s^*+1})^2 &\leq (z_1(t'_{s^*})^2 + z_2(t'_{s^*})^2) e^{\mu(t'_{s^*} - t'_{s^*+1})} + \frac{2M}{\mu} \\ &\leq (z_1(t'_{s^*})^2 + z_2(t'_{s^*})^2) e^{\mu(t'_{s^*} - t'_{s^*+1})} + \frac{\varepsilon^2}{32\bar{k}^4}. \end{aligned} \tag{4.3}$$

On the other hand, based on the switching mechanism (3.14) and the contradiction hypothesis given above, the switching happens at t'_{s^*+1}. Then, **Event ①** happens at t'_{s^*+1} and hence gives that

$$z_1(t'_{s^*+1})^2 + z_2(t'_{s^*+1})^2 > (z_1(t'_{s^*})^2 + z_2(t'_{s^*})^2) e^{\mu(t'_{s^*} - t'_{s^*+1})} + \frac{\varepsilon^2}{32\bar{k}^4},$$

which clearly contradicts (4.3). □

We are now in a position to present the main results of the paper, which are summarized in the following theorem.

Theorem 4.1. Considering system (2.2) under Assumptions 2.1-2.5, the proposed switching event-triggered controller (3.11), (3.12), (3.14) ensures the following three aspects of performance:

i) all signals of the closed-loop system are bounded on $[0, +\infty)$, while system output satisfies the output constraint on $[0, +\infty)$;

ii) system output y practically tracks the reference signal y_r;

iii) the Zeno phenomenon is excluded, i.e., all the sampling intervals have a positive lower bound, that is, there is a positive constant ϖ such that

$$\inf\{t_{k+1} - t_k\} > \varpi.$$

Proof. The proof of such theorem is divided into the following two parts.

Part I: Proof of claim *i*) By Proposition 4.2, switching of controller parameters $\hat{c}_1$, $\hat{c}_2$ happens a finite number of times. Then, **Event ①** does not happen after some times. Suppose that switching stops at t_f. Then, the following inequality holds after t_f, based on the switching mechanism:

$$z_1(t)^2 + z_2(t)^2 \leq (z_1(t_f)^2 + z_2(t_f)^2)e^{t_f - t} + \frac{\varepsilon^2}{32\bar{k}^4}, \quad t > t_f, \tag{4.4}$$

which implies that z_1, z_2 are bounded. Noting that η is bounded, the first equality of (3.5) brings the boundedness of ξ and, hence gives the boundedness of x_1 and α_1. Moreover, the second equality of (3.5), together with the boundedness of α_1, z_2, gives the boundedness of x_2, and hence those of α_2 and U.

By the switching mechanism (3.14), together with **Event ①**, on each switching interval $[t'_s, t'_{s+1})$, the following inequality holds:

$$z_1(t)^2 + z_2(t)^2 \leq z_1(t'_s)^2 + z_2(t'_s)^2 + \frac{\varepsilon^2}{32\bar{k}^4},\ t \in [t'_s, t'_{s+1}),$$

which implies the boundedness of z_1 on $[t'_s, t'_{s+1})$. This, together with the boundedness of η, gives the boundedness of ξ. Then, the output constraint is ensured on each switching interval $[t'_s, t'_{s+1})$. Therefore, for the initial output $y(0)$, which satisfies $k_l(0) \leq y(0) \leq k_u(0)$, we obtain that the output satisfies the output constraint on the first switching interval $[t'_0, t'_1)$. Subsequently, originating from $y(t'_1)$, which satisfies the output constraints, the output constraint is ensured on the next switching interval $[t'_1, t'_2)$. Consequently, the output constraint is ensured on $[0, +\infty)$ by an iterative derivation.

Part II: Proof of claim *ii*) Since $\lim_{t\to+\infty}(z_1(t_f)^2 + z_2(t_f)^2)e^{t_f - t} = 0$, there is $T > t_f$ such that $(z_1(t_f)^2 + z_2(t_f)^2)e^{t_f - t} < \frac{\varepsilon^2}{32\bar{k}^4}$, $t > T$. Then, (4.4) directly brings that

$$z_1^2 < \frac{\varepsilon^2}{16\bar{k}^4},\ t > T. \tag{4.5}$$

Moreover, since the system output y satisfies the prescribed output constraint, we have $\Phi \geq \frac{1}{4\bar{k}^2}$ from (3.10). This, together with (3.9) and (4.5), brings that $|y - y_r| = \frac{1}{\Phi}|z_1| < \varepsilon$, $t > T$. Thus, the practical tracking performance is ensured.

Part III: Proof of claim *iii*) By the sampling mechanism and the switching one given above, we know that for each sampling interval $[t_k, t_{k+1})$, there is a switching interval $[t'_s, t'_{s+1})$ such that $[t_k, t_{k+1}) \in [t'_s, t'_{s+1})$ (as analyzed in Remark 3 above). Then, the proof is given by the following two cases:

Case 1): At t'_{s+1}, controller parameters update. In such case, t'_{s+1} is also the last sampling time on $[t'_s, t'_{s+1})$. This directly excludes the Zeno phenomenon.

Case 2): At t'_{s+1}, controller parameters do not update. In such case, $t'_{s+1} = +\infty$. Then, sampling just happens at t_{k+1} when **Event ②** but not ① happens. Therefore, the following proof is given by contradiction. Suppose that the Zeno phenomenon exists. Then, the sampling happens an infinite number of times at infinitesimal time. Then, there is a $T \in [t'_s, +\infty)$, such that

$$\lim_{k\to+\infty} t_k = T, k \in \mathbf{N}_+. \tag{4.6}$$

Seeing from (3.8), we obtain that

$$\dot{\alpha}_2 = \frac{\partial\alpha_2}{\partial x_1}\xi_2 + \frac{\partial\alpha_2}{\partial x_2}\left(\theta_0 U + \sum_{j=1}^{2}\theta_j\varphi_{2,j}(x_2) + d(t)\right) + \frac{\partial\alpha_2}{\partial y_r}\dot{y}_r + \frac{\partial\alpha_2}{\partial k_l}\dot{k}_l + \frac{\partial\alpha_2}{\partial k_u}\dot{k}_u$$

which implies that $\dot{\alpha}_2$ is bounded, since all terms on the right-hand side of the above equality are bounded. Thus, there is some positive constant $\bar{M}_2$ such that $|\dot{\alpha}_2| \le \bar{M}_2$.

Define $t^* = \sup\{t \in [t_k, t_{k+1})||U - \alpha_2| = 0\}$. Then, $|U - \alpha_2| > 0$, $t \in [t^*, t_{k+1})$, and hence gives that

$$\frac{\mathrm{d}|U-\alpha_2|}{\mathrm{d}t} = \frac{\mathrm{d}\sqrt{(U-\alpha_2)^2}}{\mathrm{d}t} = \frac{(U-\alpha_2)(-\dot{\alpha}_2)}{\sqrt{(U-\alpha_2)^2}} \le |\dot{\alpha}_2| < M_1.$$

Integrating both sides of the above inequality over $[t^*, t_{k+1})$, while noting $U(t^*) - \alpha_2(t^*) = 0$, $U(t_{k+1}^-) - \alpha_2(t_{k+1}^-) = \delta$ leads to

$$\delta = \int_{t^*}^{t_{k+1}^-} \frac{\mathrm{d}|U-\alpha_2|}{\mathrm{d}t} < M_1(t_{k+1}^- - t^*),$$

which brings

$$t_{k+1} - t_k > t_{k+1} - t^* \ge \frac{\delta}{M_1}.$$

This implies that

$$t_k = t_k - t_1 = (k-1)\frac{\delta}{M_1} > T,$$

with $k > [\frac{TM_1}{\delta}] + 1$, and hence contradicts (4.6). This completes the proof. □

5. Simulation results

5.1. Simulation results using the proposed method

In this section, we demonstrate the effectiveness of the proposed theoretical results for system (2.2) with initial conditions $x_1(0) = -0.9$, $x_2(0) = -0.81$. In order to show the robustness of the proposed method to parametric uncertainties and the disturbance, the actual values of system parameters and disturbance for two cases are assumed to be as given in Table 1.

Table 1. Values of the parameters and disturbance.

Parameters/disturbance	Values (Case 1)	Values (Case 2)
θ_0	-5.5	10.5
θ_1	-80	80
θ_2	200	100
$d(t)$	$1 + \sin 2t + \cos t$	$5 + 2\sin t + 0.5\cos 2t$

Suppose that the output constraints are chosen as $k_l(t) = 3\sin\frac{t}{6} - 6$, $k_u(t) = 3\sin\frac{t}{2} + 8$. Then, for the reference signal $y_r(t) = 2 + 4\sin\frac{t}{2} - 3\cos\frac{t}{6}$ with tracking accuracy $\epsilon = 0.05$, we use a switching event-triggered controller (3.11), (3.12), (3.14) with the candidate sequences $\{C_{i,s} | s \in \mathbb{N}\}$, $i = 1, 2$ being chosen as (3.16). Consequently, 12 simulation figures are obtained for the system with two cases given by Table 1 (Figures 2–7 for Case 1 and Figures 8–13 for Case 2), which validate the effectiveness of the algorithm. Specifically, Figures 2 and 8 show that the system output enters into and then remains at the given neighborhood of the origin, while Figures 3 and 9 show that the system output always satisfies the output constraint. Figures 4, 10 and 5, 11 show that both state x_2 and control input U, respectively, are bounded. Figures 6, 12 and 7, 13 show that the two controller gains $\hat{c}_1$ and $\hat{c}_2$, respectively, remain at certain constants after a finite number of switchings.

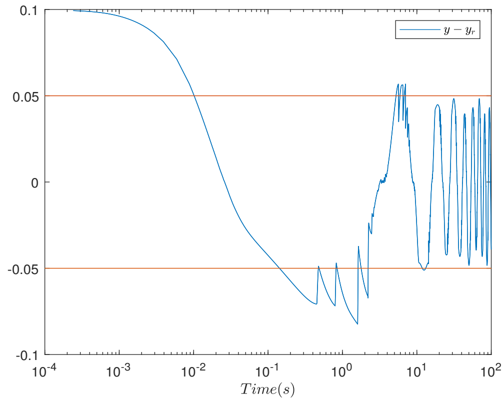

Figure 2. Trajectory of tracking error $y - y_r$ for Case 1.

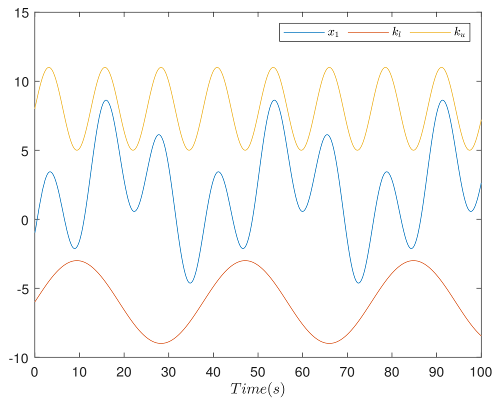

Figure 3. Trajectory of system output with constraints for Case 1.

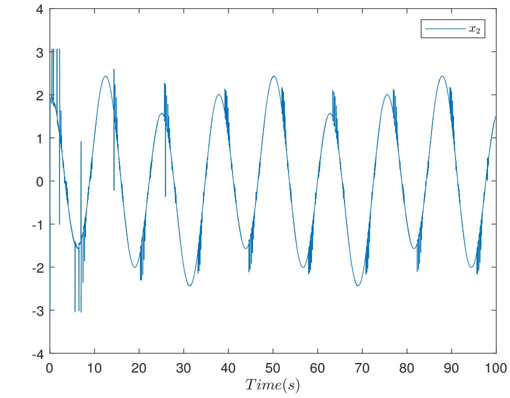

Figure 4. Trajectory of state X_2 for Case 1.

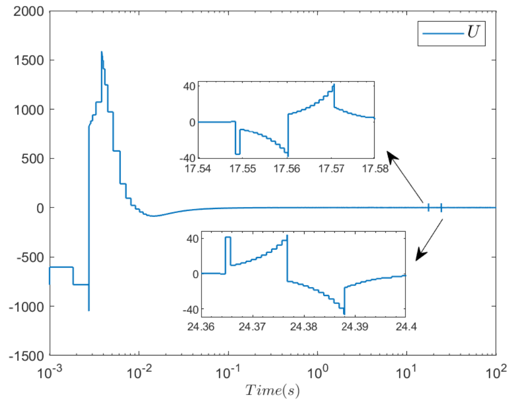

Figure 5. Trajectory of control input U for Case 1.

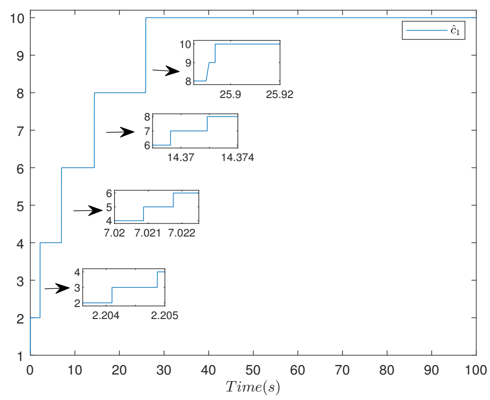

Figure 6. Trajectory of controller gain $\hat{c}_1$ for Case 1.

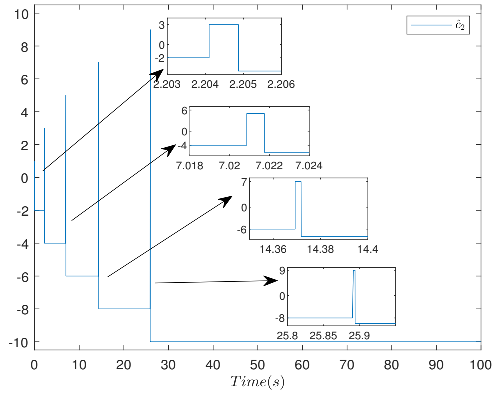

Figure 7. Trajectory of controller gain $\hat{c}_2$ for Case 1.

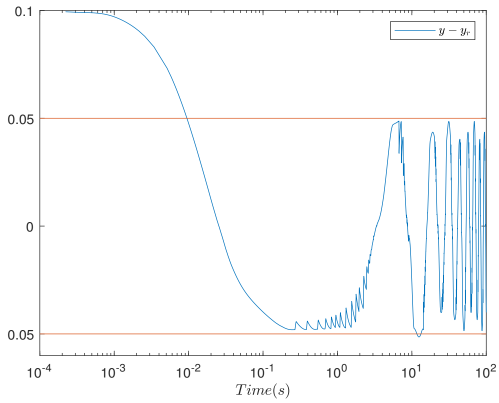

Figure 8. Trajectory of tracking error $y - y_r$ for Case 2.

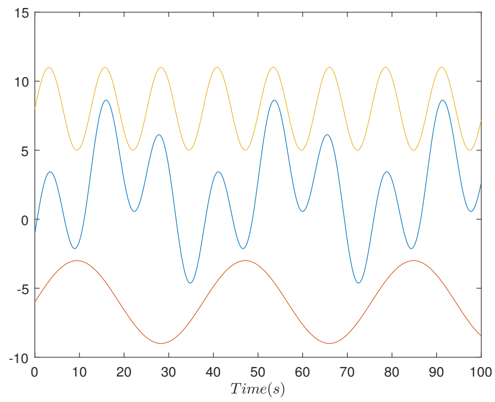

Figure 9. Trajectory of system output with constraints for Case 2.

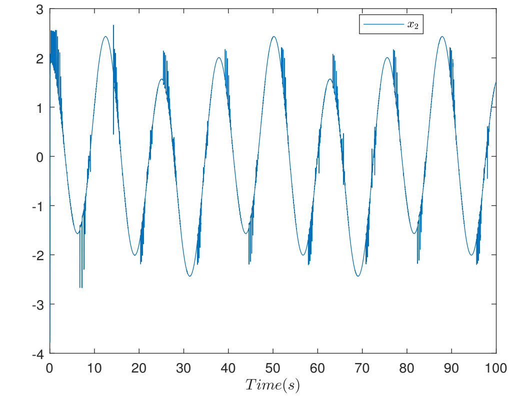

Figure 10. Trajectory of state X_2 for Case 2.

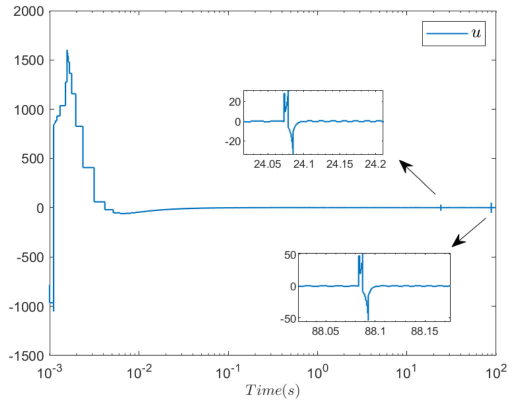

Figure 11. Trajectory of control input U for Case 2.

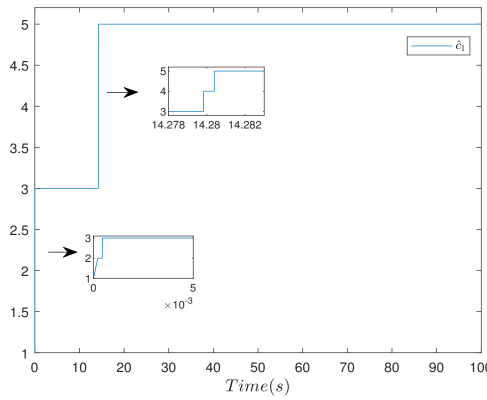

Figure 12. Trajectory of controller gain $\hat{c}_1$ for Case 2.

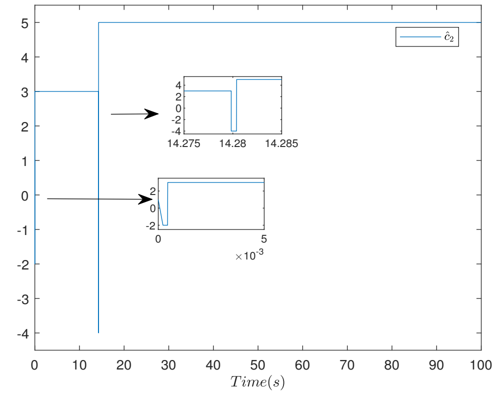

Figure 13. Trajectory of controller gain $\hat{c}_2$ for Case 2.

5.2. Comparison with PID method

Since the PID method is capable to solve the control problem under the same conditions regarding uncertainties and output constraint, while those from the related literature are not, we compare the simulation results of the proposed method and the PID. Specifically, for system (2.2) with initial conditions, output constraint, and reference signal as those in Section 5.1, we apply the PID controller with the three controller gains, i.e., proportion coefficient (P), integration (I), and differentiation (D), chosen as $P = 10$, $I = -20$, $D = 35$. Then, two simulation figures are obtained (i.e., Figures 14 and 15 for Cases 1 and 2 in Table 1, respectively).

Compared with the simulation results of the PID method, the proposed method shows stronger robustness to the parametric uncertainties and the disturbance. Specifically, for system (2.2), with different values of unknown parameters and disturbances (given by two cases in Table 1), the proposed method is effective (as shown in Figures 2–13 above). On the other hand, the PID method guarantees tracking performance only for Case 1 (as shown in Figure 14), failling for Case 2, with the same controller gains (as shown in Figure 15).

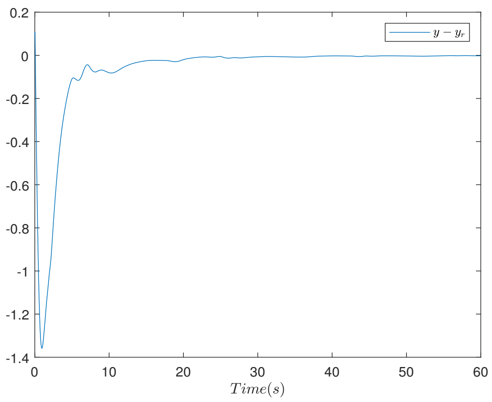

Figure 14. Trajectory of tracking error $y - y_r$ for Case 1 by PID.

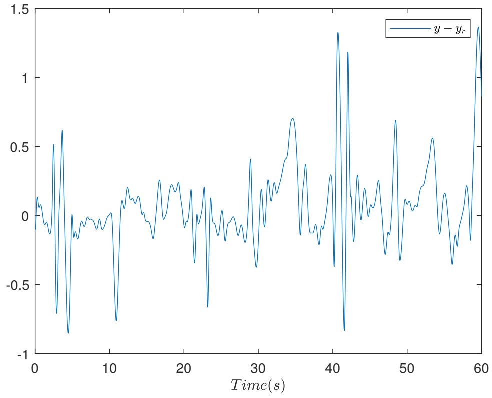

Figure 15. Trajectory of tracking error $y - y_r$ for Case 2 by PID.

6. Conclusions

In this paper, a switching event-triggered control scheme is proposed for the course tracking control of a class of SVs with output constraint and unknown control direction. By the proposed scheme, an event-triggered controller is designed, together with two mechanisms, one for the sampling of the controller and , and the other for the switching of controller parameters. It is proved that the designed controller guarantees the boundedness of all states of the resulting closed-loop system, while the system output practically tracks the reference signal, along with the satisfaction of the output constraint and the exclusion of the Zeno phenomenon. Noting the fact that all states must be available for feedback in the proposed controller, future research will focus on the output feedback control for the investigated system, i.e., when only the course angle of the SV is observed. To solve such control problem, a state observer should be designed to reconstruct the unmeasurable states together with the design of a switching and event-triggered mechanism. Then, a new control framework should be established, which will be essentially different, and challenges the control problem under investigation.

Author contributions

Qian Gao: Wrote the manuscript, conducted simulations, formal analysis; Jian Li: Writing-review and editing. All authors have read and approved the final version of the manuscript for publication.

Use of Generative-AI tools declaration

The authors declare they have not used Artificial Intelligence (AI) tools in the creation of this article.

Acknowledgments

This work was supported by the National Natural Science Foundations of China (62473325).

Conflict of interest

The authors declare that they have no conflicts of interest.

References

1. M. M. Islam, S. A. Siffat, I. Ahmad, M. Liaquat, Robust integral backstepping and terminal synergetic control of course keeping for ships, *Ocean Eng.*, **221** (2021), 108532. https://doi.org/10.1016/j.oceaneng.2020.108532
2. H. Zhang, X. Zhang, R. Bu, Active disturbance rejection control of ship course keeping based on nonlinear feedback and ZOH component, *Ocean Eng.*, **233** (2021), 109136. https://doi.org/10.1016/j.oceaneng.2021.109136
3. N. Wang, S. Lv, Z. Liu, Global finite-time heading control of surface vehicles, *Neurocomputing*, **175** (2016), 662–666. https://doi.org/10.1016/j.neucom.2015.10.106
4. Z. Gao, G. Guo, Command filtered finite/fixed-time heading tracking control of surface vehicles, *IEEE-CAA J. Autom. Sin.*, **8** (2021), 1667–1676. https://doi.org/10.1109/JAS.2021.1004135
5. J. Ning, Y. Ma, L. Liu, T. Li, Fuzzy course tracking control of an unmanned surface vehicle with event-triggered mechanism and input quantization, *Ocean Eng.*, **288** (2023), 115704. https://doi.org/10.1016/j.oceaneng.2023.115704
6. X. Zhang, X. Xu, J. Li, Y. Luo, G. Wang, G. Brunauer, et al., Observer-based H_∞ fuzzy fault-tolerant switching control for ship course tracking with steering machine fault detection, *ISA Trans.*, **140** (2023), 32–45. https://doi.org/10.1016/j.isatra.2023.05.021
7. Q. Wang, Y. Guan, J. Ning, L. Hao, Y. Yin, Neural network-based adaptive dynamic surface course tracking control of an unmanned surface vehicle with signal input quantization, *Int. J. Adapt. Control*, **39** (2025), 1731–1743. https://doi.org/10.1002/acs.4017
8. Z. Dong, T. Bao, M. Zheng, X. Yang, L. Song, Y. Mao, Heading control of unmanned marine vehicles based on an improved robust adaptive fuzzy neural network control algorithm, *IEEE Access*, **7** (2019), 9704–9713. https://doi.org/10.1109/ACCESS.2019.2891106
9. P. Li, W. Bai, W. Zhang, Y. Xv, Reinforcement learning-based optimal control for USVs course tracking under disturbances, *J. Intell. Robot. Syst.*, **111** (2025), 83. https://doi.org/10.1007/s10846-025-02281-w
10. R. Wu, J. Du, Adaptive robust course-tracking control of time-varying uncertain ships with disturbances, *Int. J. Control Autom. Syst.*, **17** (2019), 1847–1855. http://dx.doi.org/10.1007/s12555-018-0733-2
11. J. Wu, C. Zeng, Y. Hu, Indirect adaptive robust control design for course tracking of ships subject to unknown control coefficient and disturbances, *Int. J. Control Autom. Syst.*, **19** (2021), 2059–2067. http://dx.doi.org/10.1007/s12555-020-0052-2
12. J. Du, X. Hu, Y. Sun. Adaptive robust nonlinear control design for course tracking of ships subject to external disturbances and input saturation, *IEEE Trans. Syst. Man Cybern. Syst.*, **50** (2017), 193–202. https://doi.org/10.1109/TSMC.2017.2761805

13. Q. Zhang, M. Zhang, Y. Hu, G. Zhu, Error-driven-based adaptive nonlinear feedback control of course-keeping for ships, *J. Mar. Sci. Technol.*, **26** (2021), 357–367. https://doi.org/10.1007/s00773-020-00741-6
14. Z. Gao, G. Guo, Adaptive heading tracking control of surface vehicles with unknown control directions and full state constraints, *Neurocomputing*, **359** (2019), 517–525. https://doi.org/10.1016/j.neucom.2019.06.091
15. Z. Li, W. Xu, J. Yu, C. Wang, G. Cui, Finite-time adaptive heading tracking control for surface vehicles with full state constraints, *IEEE Trans. Circuits Syst. II Express Briefs*, **69** (2021), 1134–1138. https://doi.org/10.1109/TCSII.2021.3099491
16. Y. Yue, J. Ning, T. Li, L. Liu, Adaptive neural network course tracking control of USV with input quantisation and output constraints, *Int. J. Syst. Sci.*, **56** (2025), 2674–2688. https://doi.org/10.1080/00207721.2025.2454413
17. Y. Liu, Y. Sun, L. Hao, Nonsingular finite-time heading tracking control of marine vehicles with tracking error constraints, *J. Frankl. Inst.*, **361** (2024), 106734. https://doi.org/10.1016/j.jfranklin.2024.106734
18. P. Tallapragada, N. Chopra, On event triggered tracking for nonlinear systems, *IEEE Trans. Autom. Control*, **58** (2013), 2343–2348. https://doi.org/10.1109/TAC.2013.2251794
19. L. Xing, C. Wen, Z. Liu, H. Su, J. Cai, Event-triggered adaptive control for a class of uncertain nonlinear systems, *IEEE Trans. Autom. Control*, **62** (2016), 2071–2076. https://doi.org/10.1109/TAC.2016.2594204
20. F. Li, Y. Liu. Adaptive event-triggered output-feedback controller for uncertain nonlinear systems, *Automatica*, **117** (2020), 109006. https://doi.org/10.1016/j.automatica.2020.109006
21. X. Zhao, H. Wu, J. Cao, L. Wang, Prescribed-time synchronization for complex dynamic networks of piecewise smooth systems: A hybrid event-triggering control approach, *Qual. Theory Dyn. Syst.*, **24** (2025), 11. https://doi.org/10.1007/s12346-024-01166-x